

# Effects of helium ion bombardment on metallic gold and iridium thin films

Sara Zuccon,<sup>1</sup> Enrico Napolitani,<sup>3</sup> Enrico Tessoro,<sup>1</sup> Paola Zuppella,<sup>1</sup> Alain J. Corso,<sup>1</sup>  
F. Gerlin,<sup>1</sup> M. Nardello<sup>1,2</sup> and Maria G. Pelizzo<sup>1,2,\*</sup>

<sup>1</sup>CNR-IFN UOS Padova, Via Trasea 7, I-35131, Padova

<sup>2</sup>University of Padova, Department of Information Engineering, Via Gradenigo 6/b, I-35131, Padova, Italy

<sup>3</sup>CNR-IMM MATIS and Dipartimento di Fisica e Astronomia, Università di Padova, via Marzolo 8, I-35131, Padova, Italy

\*pelizzo@dei.unipd.it

**Abstract:** Single layer mirrors have been prepared by evaporating gold and iridium on silicon substrates. The samples have been exposed to 4 keV He<sup>+</sup> ion flux at different total fluences, simulating the effect of solar wind ions on optical coatings. We show that the ion implantation significantly affects the optical characteristics of the metallic films. The phenomena are explained and modeled also considering the related material modifications observed with chemical and morphological analysis.

©2014 Optical Society of America

**OCIS codes:** (310.0310) Thin films; (120.6085) Space instrumentation; (160.0160) Materials; (230.4040) Mirrors; (260.7210) Ultraviolet.

---

## References and links

1. E. Marsch, R. G. Marsden, R. A. Harrison, R. Wimmer-Schweingruber, and B. Fleck, "Solar Orbiter—mission profile, main goals and present status," *Adv. Space Res.* **36**(8), 1360–1366 (2005).
2. E. Antonucci, S. Fineschi, G. Nalletto, M. Romoli, D. Spadaro, G. Nicolini, P. Nicolosi, L. Abbo, V. Andretta, A. Bemporad, F. Auchère, A. Berlicki, R. Bruno, G. Capobianco, A. Ciaravella, G. Crescenzo, V. Da Deppo, R. D'Amicis, M. Focardi, F. Frassetto, P. Heinzl, P. L. Lamy, F. Landini, G. Massone, M. A. Malvezzi, J. D. Moses, M. Pancrazzi, M. G. Pelizzo, L. Poletto, U. H. Schühle, S. K. Solanki, D. Telloni, L. Teriaca, and M. Uslenghi, "Multi Element Telescope for Imaging and Spectroscopy (METIS) coronagraph for the Solar Orbiter mission," *Proc. SPIE* **8443**, 844309 (2012).
3. S. Fineschi, E. Antonucci, G. Nalletto, M. Romoli, D. Spadaro, G. Nicolini, P. Nicolosi, L. Abbo, V. Andretta, A. Bemporad, F. Auchère, A. Berlicki, R. Bruno, G. Capobianco, A. Ciaravella, G. Crescenzo, V. Da Deppo, R. D'Amicis, M. Focardi, F. Frassetto, P. Heinzl, P. L. Lamy, F. Landini, G. Massone, M. A. Malvezzi, J. D. Moses, M. Pancrazzi, M. G. Pelizzo, L. Poletto, U. H. Schühle, S. K. Solanki, D. Telloni, L. Teriaca, and M. Uslenghi, "METIS: a novel coronagraph design for the Solar Orbiter mission," *Proc. SPIE* **8443**, 84433H (2012).
4. A. Ziani, F. Delmotte, C. Le Paven-Thivet, E. Meltchakov, A. Jerome, M. Roulliy, F. Bridou, and K. Gasc, "Ion beam sputtered aluminum based multilayer mirrors for extreme ultraviolet solar imaging," *Thin Solid Films* **552**, 62–67 (2014).
5. ESA, "Solar Orbiter environmental specification - Issue 3.0," (2010).
6. A. D. Rousseau, D. L. Windt, B. Winter, L. Harra, H. Lamoureux, and F. Eriksson, "Stability of EUV multilayers to long-term heating, and to energetic protons and neutrons, for extreme solar missions," *Proc. SPIE* **5900**, 590004 (2005).
7. G. Nalletto, A. Boscolo, J. Wyss, and A. Quaranta, "Effects of proton irradiation on glass filter substrates for the Rosetta mission," *Appl. Opt.* **42**(19), 3970–3980 (2003).
8. I. Di Sarcina, M. L. Grilli, F. Menchini, A. Piegari, S. Scaglione, A. Sytchkova, and D. Zola, "Behavior of optical thin-film materials and coatings under proton and gamma irradiation," *Appl. Opt.* **53**(4), A314–A320 (2014).
9. M. Nardello, P. Zuppella, V. Polito, A. J. Corso, S. Zuccon, and M. G. Pelizzo, "Stability of EUV multilayer coatings to low energy alpha particles bombardment," *Opt. Express* **21**(23), 28334–28343 (2013).
10. M. G. Pelizzo, A. J. Corso, P. Zuppella, D. L. Windt, G. Mattei, and P. Nicolosi, "Stability of extreme ultraviolet multilayer coatings to low energy proton bombardment," *Opt. Express* **19**(16), 14838–14844 (2011).
11. A. S. Kuznetsov, M. A. Gleeson, and F. Bijkerk, "Ion effects in hydrogen-induced blistering of Mo/Si multilayers," *J. Appl. Phys.* **114**(11), 113507 (2013).
12. A. S. Kuznetsov, M. A. Gleeson, and F. Bijkerk, "Hydrogen-induced blistering of Mo/Si multilayers: Uptake and distribution," *Thin Solid Films* **545**, 571–579 (2013).

13. V. Rigato, A. Patelli, G. Maggioni, G. Salmaso, V. Mattarello, M. G. Pelizzo, P. Nicolosi, L. Depero, E. Bontempi, and P. Mazzoldi, "Effects of ion bombardment and gas incorporation on the properties of Mo/a-Si:H multilayers for EUV applications," *Surf. Coat. Tech.* **174–175**, 40–48 (2003).
14. R. Livengood, S. Tan, Y. Greenzweig, J. Notte, and S. McVey, "Subsurface damage from helium ions as a function of dose, beam energy, and dose rate," *J. Vac. Sci. Technol. B: Microelectronics and Nanometer Structures* **27**(6), 3244 (2009).
15. V. Ranieri, M. Saggio, and E. Rimini, "Voids in silicon by He implantation: From basic to applications," *J. Mater. Res.* Vol **15**(7), 1449–1477 (2000).
16. J. F. Ziegler and J. P. Biersack, *SRIM - The Stopping and Range of Ions in Solids* (Pergamon Press, 1985).
17. V. Veligura, G. Hlawacek, R. P. Berkelaar, R. van Gastel, H. J. W. Zandvliet, and B. Poelsema, "Digging gold: keV He<sup>+</sup> ion interaction with Au," *Beilstein J Nanotechnol* **4**, 453–460 (2013).
18. P. Zuppella, G. Monaco, A. J. Corso, P. Nicolosi, D. L. Windt, V. Bello, G. Mattei, and M. G. Pelizzo, "Iridium/silicon multilayers for extreme ultraviolet applications in the 20–35 nm wavelength range," *Opt. Lett.* **36**(7), 1203–1205 (2011).
19. G. Naletto, M. G. Pelizzo, G. Tondello, S. Nannarone, and A. Giglia, "The monochromator for the synchrotron radiation beamline X-MOSS at ELETTRA," *Proc. SPIE*, Vol. **4145**, p. 105 (2001).
20. S. Nannarone, F. Borgatti, A. DeLuisa, B. P. Doyle, G. C. Gazzadi, A. Giglia, P. Finetti, N. Mahne, L. Pasquali, M. Pedio, G. Selvaggi, G. Naletto, M. G. Pelizzo, and G. Tondello, "The BEAR beamline at ELETTRA," *AIP Conf. Proc.* **705**, 450–453 (2004).
21. A. Benninghoven, F. G. Rüdener, and H. W. Werner, *Secondary Ion Mass Spectrometry* (Wiley, 1987).
22. M. Seita, A. Reiser, and R. Spolenak, "Ion-induced grain growth and texturing in refractory thin films – A low temperature process," *Appl. Phys. Lett.* **101**(25), 251905 (2012).
23. G. A. Niklasson, C. G. Granqvist, and O. Hunderi, "Effective medium models for the optical properties of inhomogeneous materials," *Appl. Opt.* **20**(1), 26–30 (1981).
24. *Handbook of Optical Constants of Solids*, Edward D. Palik, ed. (Academic Press, Inc. 1985).

## 1. Introduction

Space exploration is linked to the development of increasingly innovative instrumentation, able to withstand the operation environment. In particular, new missions, like e.g. Solar Orbiter [1], foresee solar probes approaching the Sun as never before, with instrumentation operating in a harsh environment [2–4], rich in ion particles and characterized by high temperatures. Low energy alpha particles, being a major constituent of the quiet solar wind next to protons, are considered one of the major causes of potential damage of the optical instrumentation and components [5]. While there are many studies related to the interaction of high energy ions in space (of the order of MeV), in particular protons [6–8], only very recently experiments with low energy particles (of the order of keV) have been reported [9, 10]. An experiment with different material thin films used for mirror fabrication implanted with 60 keV protons demonstrated that, due to the short penetration of the low energy ions, they are implanted inside the coatings themselves, changing their optical properties [8]; such changes depend on the different materials under consideration. Concerning the optical properties, the variation of the refractive index has been considered to describe the overall effect. First experiments on multilayer mirrors optical coatings bombarded with low energy protons (1 keV) and alpha particles (4 keV) have been recently reported, demonstrating that such ion implantation causes delamination [9] and/or interface intermixing [10]. Such effects are also reported in thin film structures for Extreme UltraViolet Lithography (EUVL) demonstrating that low energy hydrogen ions are responsible for the formation of blisters and layers detachment in nanoscale Mo/Si multilayers [11–13]. The induced damage of helium atoms on semiconductor materials has also been studied, in order to verify the potential damage of samples in ion microscopy [14, 15] showing that low energy ions cause formation of surface nanobubbles. The effect strongly depends on the material characteristics, suggesting that each material presents different damage regimes as a function of energy and ion fluence. In particular SEM analysis on copper samples have shown that nanobubbles are confined within a subsurface region of about few tens of nanometers in case of 12 keV He, with ion and damage depth profiles showing a consistent 20–30 nm offset compared to Stopping and Range of Ions in Matter (SRIM) [16] simulations. While most of the studies relates to silicon and other semiconductor materials, a specific experimental study of the interaction of He<sup>+</sup> with Au (111) has been carried out using ion energies between 15 and 35

keV and fluences above  $1 \times 10^{17} \text{cm}^{-2}$  [17]. It has been demonstrated that at lower energies the implantation lead to the formation of subsurface bubbles that quickly reach the surface releasing the helium, and developing a sponge like surface. At 35 keV nanobubbles form in the deeper part of the film and then grow with the fluence, such that for a total fluence of  $4.8 \times 10^{17} \text{cm}^{-2}$  formation of large blisters is observed.

In the present study, implantation of low energy 4 keV He + ions has been carried out on iridium and gold thin films on silicon substrates. Such materials have been selected since they are widely use as mirror coatings for high reflectance in the vacuum ultraviolet (VUV) and visible (VIS) spectral range. Helium implantation of these coatings has not been investigated before at such low energies. The implantation parameters have been chosen to simulate the solar wind effect in this interplanetary environment close to the Sun. During a space mission such as Solar Orbiter it is necessary to consider fluences equivalent to 1 year, 2 years, and 4 years of mission time. According to [17], energy and total fluence should be below the limit of formation of nanobubbles leading to blistering. Reflectance measurements have been compared with morphological and chemical characterization. In particular, atomic force microscopy (AFM) has been done in order to check for any surface degradation or blistering. Chemical depth profiling have been performed with Secondary Ion Mass Spectrometry (SIMS) in order to verify the depth distribution of helium atoms inside the samples and to check for the presence of other contaminants. The change of reflectance performances of such thin films in the visible and in the ultraviolet spectral region has been experimentally evaluated and then it has been explained in terms of a variation of the refractive index caused by the implantation. SIMS measurements coupled with SRIM simulations confirms such model. The results of this study represents a fundamental step in understanding the degradation process on optical coatings, thus in developing strategies to avoid such degradation or to mitigate it, in order to develop new generation optical components capable to withstand the new space frontiers environments.

## 2. Materials and methods

Silicon substrates are Czochralski grown p-type Si polished wafer, 650–700  $\mu\text{m}$  thick. Gold mirrors have been prepared by electron-beam vapor deposition starting from 99.99% pure gold pellets (Kurt J. Lesker Company). A thin layer of Chromium (2 nm) has been deposited as adhesion layer. The gold film is 220 nm thick. Iridium mirrors have been acquired by RXO LLC; again, on a Si polished wafer an Ir thin film coating, of thickness 80 nm, was deposited by RF-magnetron sputtering [18]. Two samples (Au0 and Ir0) were kept unexposed, to be the reference ones. The other samples have been exposed to low energy He + ions in three different sessions. This ion implantation has been performed at the Forschungszentrum Dresden-Rossendorf (Germany, ex Helmholtz-Zentrum Dresden-Rossendorf) in the Low Energy Implanter (LEI) facility. The fluences have been chosen in order to simulate the effects of respectively 1 year, 2 years and 4 years mission. The experimental parameters, such as samples label, fluences, fluxes and energies, are listed in Table 1 [9].

**Table 1. Ion implantation experimental parameters.**

	Samples Au1 and Ir1 (1 year fluence)	Samples Au2 and Ir2 (2 years fluence)	Samples Au4 and Ir4 (4 years fluence)
Duration	5h	10 h	20 h
He + energy	4 keV	4 keV	4 keV
He + flux	$1.5 \cdot 10^{11} \text{ s}^{-1} \text{cm}^{-2}$	$1.5 \cdot 10^{11} \text{ s}^{-1} \text{cm}^{-2}$	$1.5 \cdot 10^{11} \text{ s}^{-1} \text{cm}^{-2}$
Total fluence	$2.6 \cdot 10^{15} \text{ He}^+/\text{cm}^2$	$5.2 \cdot 10^{15} \text{ He}^+/\text{cm}^2$	$1.1 \cdot 10^{16} \text{ He}^+/\text{cm}^2$

During the experiment, the chamber pressure was kept constantly lower than  $10^{-8}$  mbar and the temperature within  $27^{\circ}\text{C} - 29^{\circ}\text{C}$ . The samples were kept perpendicularly to the He<sup>+</sup> ion flux. The ion current was integrated over time in order to control the total fluence. The reflectance of the samples prior and after exposure has been tested in three different spectral regions:

- In the visible range (300 nm – 800 nm);
- In the VUV range wavelength near the Lyman- $\alpha$  line of the solar emission spectrum (121.6 nm);
- In the VUV region between 48 nm and 66 nm (only on Ir).

The reflectance in the visible spectral range has been measured at the UV-VIS-NIR spectrophotometer Cary 5000, with the variable angle specular reflectance accessory (VASRA) at  $20^{\circ}$  of incidence. The performances in the VUV been tested at the Bending Magnet for Emission Absorption and Reflectivity (BEAR) beamline at ELETTRA Synchrotron (Trieste, Italy) [19, 20]. The measurements have been performed at  $5^{\circ}$  incidence, using a 0.9 polarized beam. The morphology of the samples, both irradiated and not irradiated, has been characterized by using Atomic Force Microscope operating in non-contact mode (XE-70, Park System), in order to verify a possible change of the surface morphology due to the ion bombardment.

The ion implantation profiles have been experimentally determined by SIMS measurements on samples Au<sub>4</sub> and Ir<sub>4</sub> and on the corresponding reference samples. Measurements have been done by sputtering the samples with a 10 nA, 5.5 keV Cs<sup>+</sup> beam, while collecting CsHe<sup>+</sup>, CsO<sup>+</sup>, CsSi<sup>+</sup>, CsCr<sup>+</sup> secondary ions from a central area of the sputtering crater. Erosion time vs depth calibration has been done by measuring the crater depth after sputtering with a TENCOR P10 stylus profilometer and assuming a constant erosion rate [21]. Simulations of collision dynamics has been performed with SRIM software [16]. The software performs Montecarlo simulations of elastic scattering interactions between the incident ions and the target atoms and provides data on implanted atoms and damage depth distributions, as well as surface sputtering. He<sup>+</sup> ions energy of 4 keV has been specified and a statistics of total 99999 incident ions has been used.

### 3. Results and discussion

Results of reflectance measurements performed on all the samples are presented in Fig. 1 and Fig. 2 for the Au layers and in Fig. 3, Fig. 4 and Fig. 5 for the Ir layers respectively. The error on the measurements can be assumed around 1% in all ranges. The experimental data show an overall reflectance decrease in both type of coatings with the increase of the ion fluence; the effect is more pronounced in the VUV spectral range. Degradation of optical coatings is therefore expected in space.

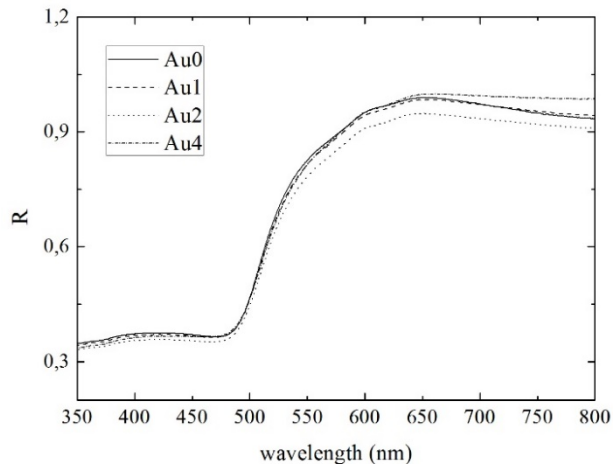


Fig. 1. Reflectance of gold mirrors in the visible spectral range.

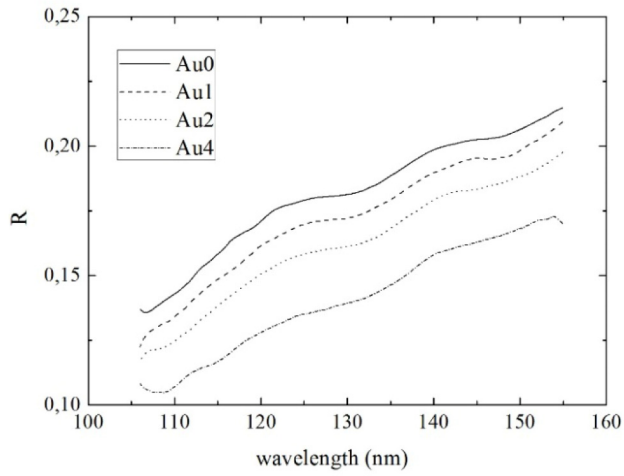


Fig. 2. Reflectance of gold mirrors in the VUV range.

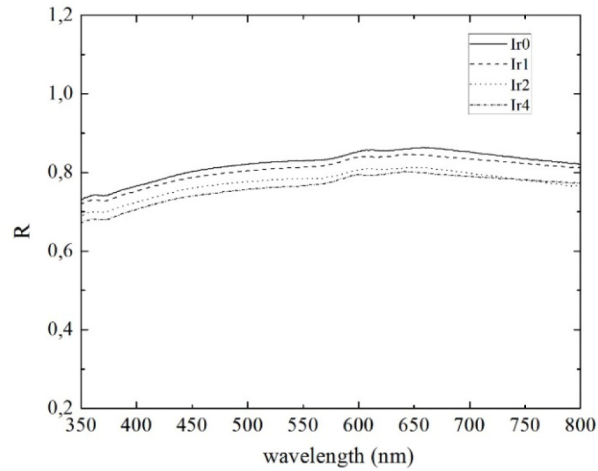


Fig. 3. Reflectance of Iridium mirrors in the visible range.

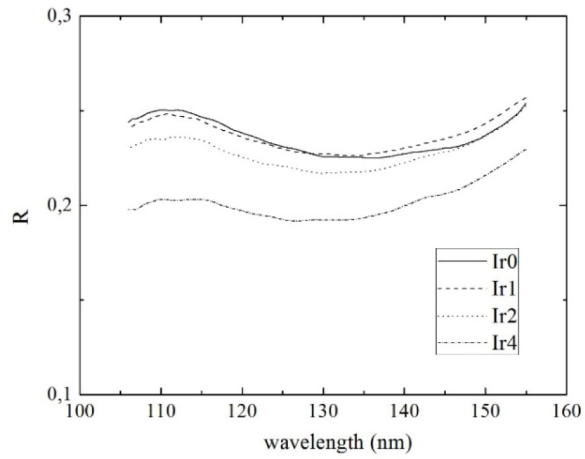


Fig. 4. Reflectance of iridium mirrors in the VUV 105-155 nm spectral range.

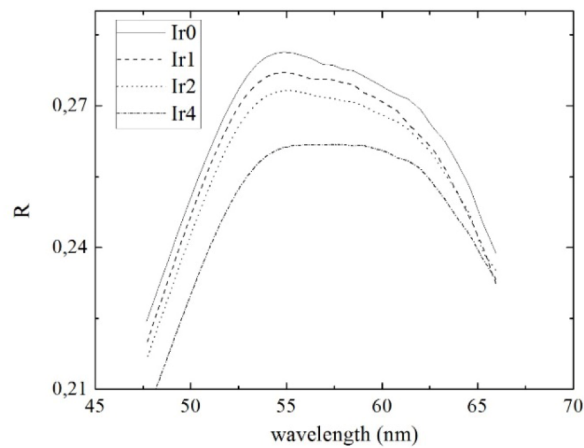


Fig. 5. Reflectance of iridium mirrors in VUV 48-66 nm spectral range.

AFM image of Au0 and Au4 surfaces are shown in Fig. 6 and Fig. 7. The images show that there is not an increase of the roughness value, but rather a slight reduction. The RMS roughness for the virgin sample is in fact 1.98 nm, while after implantation of the highest fluence it becomes 1.4 nm. Correspondingly, the grain size increases from 69 nm for the pristine gold to 132 nm for the 4-years fluence irradiated sample. This might be explained by the fact that ions release energy to the surface, increasing adatom's mobility, thus creating larger grain size [22] and reducing the roughness. In case of iridium such effect is not noticeable from AFM images, since roughness is very low and the grain size very small (around 8 nm). The change observed in Au morphology might be responsible also for the anomalous behavior in the trend of reflectance spectra above 650 nm (see Fig. 1). The pristine gold curve in this region lies below the curve of Au4 irradiated gold, while in the VUV (Fig. 2) there is a linear decrease of the reflectance with the total fluence. This might be ascribed to a plasmonic effect of the light coupling with surfaces having different morphologies. In particular, gold shows this effect above its proper resonance above 520 nm, while iridium above 200 nm, the exact position depending on the morphology.

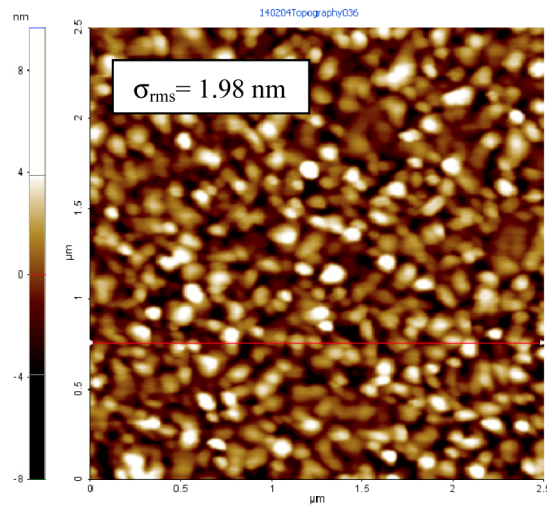


Fig. 6. AFM image of the surface of sample Au0.

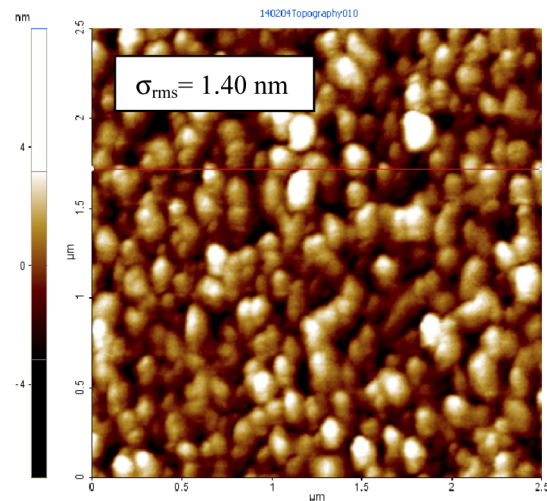


Fig. 7. AFM image of the surface of sample Au4.

Figure 8 and Fig. 9 report the SIMS depth profiles of He after implantation at the highest dose in Au and Ir samples respectively (samples Au4 and Ir4). He implantation profiles calculated with SRIM are also reported for comparison. It is clear that the experimental profiles deviate from the simulated ones. In the case of Au, in order to match the SIMS profile the density of the material was varied. It is clear that a better match is obtained with the density of  $18 \text{ gr/cm}^3$ , which is lower with respect to the normal density of Au of  $19.3 \text{ gr/cm}^3$ . Such a relatively small density reduction might be ascribed to the damage produced by the He implantation.

In the case of Ir4 (Fig. 9) a shift between SIMS and SRIM profiles is instead observed [14]. A surface sputtering occurring during He implantation might readily account for such shift. The Sputtering Yield obtained by SRIM simulations gives the average number of atoms of the target material sputtered for each incident ion. It is directly related to the surface binding energy (SBE), which is in fact an input parameter for the calculation. In Table 2, such results are reported assuming the available values of SBE in Ir and Au. In none of the cases considered in our experiment, high sputtering is expected, and the Ir has a Sputtering Yield even lower than Au. However, SBE is very sensitive to surface roughness and damage, so that it is lower for rough samples and can decrease during the bombardment because of damage and/or roughening. Roughening can be excluded as a possible source for SBE reduction, as surface roughness in our samples is relatively low and tends to reduce during He implantation (Figs. 6 and 7). However, we cannot exclude that the damage induced by He implantation, presumably in the form of very small vacancy clusters, in the case of Ir induces an anomalous reduction of SBE and consequently a significant surface sputtering. This phenomenon might be relevant for space applications and demands further investigations that will be the subject of a future work.

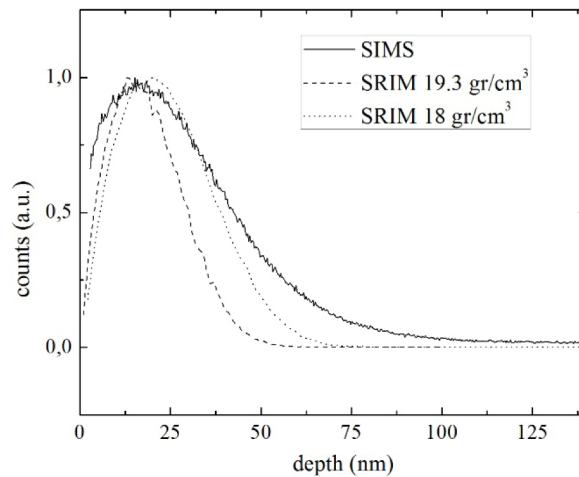


Fig. 8. Comparison between SIMS experimental data of He + distribution in gold Au4 sample and SRIM calculation assuming two different Au densities.



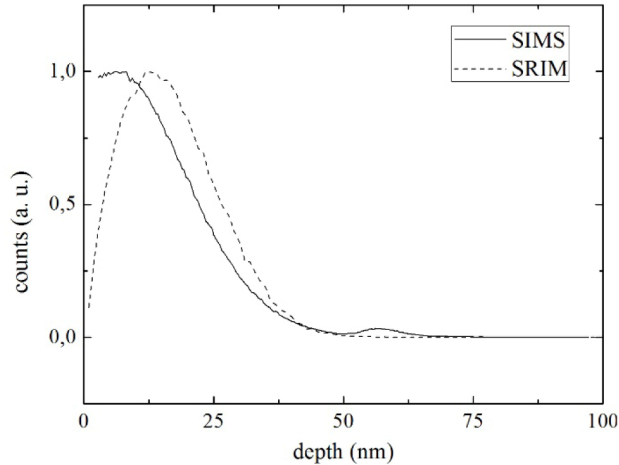


Fig. 9. Comparison between SIMS experimental data of He distribution in iridium Ir4 sample and SRIM calculation.

**Table 2. SRIM calculation main results.**

	Sputtering Yield (Atoms/Ion)	Ion Projected Range (nm)
Gold	0.19	18.3 (19.5 for less dense Au)
Iridium	0.13	16.7

An effective medium approximation (EMA) approach has been used to evaluate the influence of implanted helium on the optical properties of the mirrors. The ratio between the number of helium atoms in the implanted region and the number of gold atoms has to be estimated. In order to recover such values, the number of gold atoms for each square centimeter,  $N$ , has to be calculated firstly. The density of bulk gold is  $19.32 \text{ gr/cm}^3$  and the atomic weight of a gold atom is  $196.97 \text{ amu}$ , this implies that the density of atoms is  $5.92 \times 10^{22} \text{ cm}^{-3}$ . If intermixing thickness is assumed to be  $35 \text{ nm}$  ( $\sim$ FWHM by SIMS),  $N = 2.1 \times 10^{17} \text{ Au/cm}^2$ . On the other side, the He + 3rd total fluence is  $1.1 \times 10^{16} \text{ He}^+/\text{cm}^2$ . The fraction of the helium atoms with respect to the gold is sufficiently small to allow the application of the Maxwell-Garnett formula (MG) [23] for the calculation of the effective refractive index in the intermixing region. This formula gives the effective dielectric function,  $\epsilon_f$ , of a binary system as a function of the dielectric constant of the matrix medium (in this case gold),  $\epsilon_m$ , the constant of the inclusions (helium),  $\epsilon_{He}$ , and the volume fraction of the inclusions with respect to the matrix medium,  $v_f$ .

$$\epsilon_f = \epsilon_m \frac{2(1-v_f)\epsilon_m + (1+2v_f)\epsilon_{He}}{(2+v_f)\epsilon_m + (1-v_f)\epsilon_{He}} \quad (1)$$

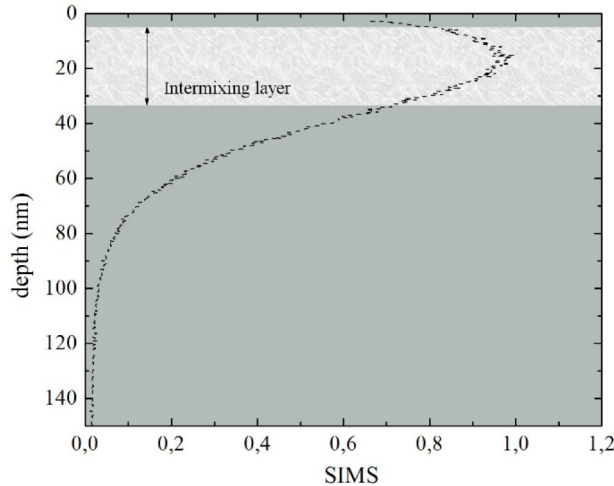


Fig. 10. Layout of the Au film where the region of major ion implanted intermixing region is highlighted. The SIMS profile is superimposed.

The reflectance of a stack of layers as the one depicted in Fig. 10, i.e. metal/intermixing/metal/silicon substrate can thus be calculated. In this first approach, the optical constant from Palik [24] have been adopted for gold, iridium and silicon, while for He the optical constant has been assumed constant over the whole range and equal to 1. The MG formula has been used to calculate the effective refractive index at each wavelength. The reflectance has been computed for different  $v_f$  with a standard transfer matrix formalism and results compared with the reflectance of a pure metal mirror (Fig. 11 and Fig. 12). This comparison has been carried out at  $5^\circ$  in the VUV spectral range, and  $20^\circ$  in the visible, as used during experimental session. The intermixing region is estimated from the FWHM of the SIMS curve (35 nm for Au and 20 nm for Ir). The volume fraction ( $v_f$ ) considered in this example is equal to 0.1, as it seems to be a value possible for both materials.

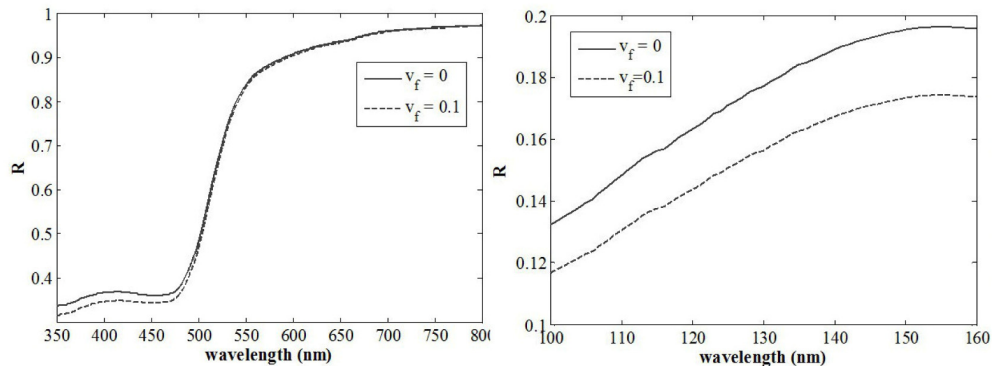


Fig. 11. Calculated reflectance for Au film with (dotted line) and without (continuous line) intermixing layer. The two wavelength ranges VUV and Visible are shown.

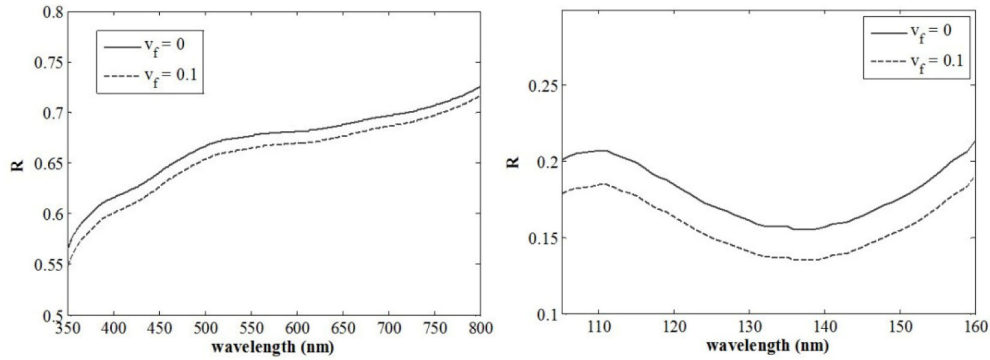


Fig. 12. Calculated reflectance for Ir film with (dotted line) and without (continuous line) intermixing layer. The two wavelength ranges EUV and visible are shown.

These calculations show that the effect of the change in refractive index caused by void in the structure is mainly observed as a decrease in reflectance, in accordance with the experimental results. In the visible region, gold shows a much smaller decrease in reflectance compared to the VUV region, slightly detectable above 500 nm. This is also in accordance with the experimental results. We have carried out a deeper analysis at 121.6 nm Ly-alpha wavelength, by computing the  $v_f$  values for which the theoretical model predicts the same relative drop of reflectance experimentally observed. In Table 3 for each fluence two values are reported. The first is the percentage drop in reflectance observed experimentally at 121.6 nm; the second is the volume fraction, which is necessary to insert into the model to recover the same decrease in reflectance as the one observed in the experimental results.

**Table 3. The experimental decrease in reflectance and the correspondent  $v_f$  are listed as function of the fluence.**

Fluence (equivalent years)	Gold		Iridium	
	Experimental R decrease (%)	correspondent $v_f$	Experimental R decrease (%)	correspondent $v_f$
0	0	0	0	0
1	-0,06	0,05	-0,01	0,018
2	-0,12	0,105	-0,05	0,04
4	-0,25	0,21	-0,16	0,11

The experimental reflectance decreases linearly as function of the fluence. The same linearity is encountered also in the correspondent volume fraction values. This is clearly represented in the graph of Fig. 13, where also the slope of the linear regression curve is reported.

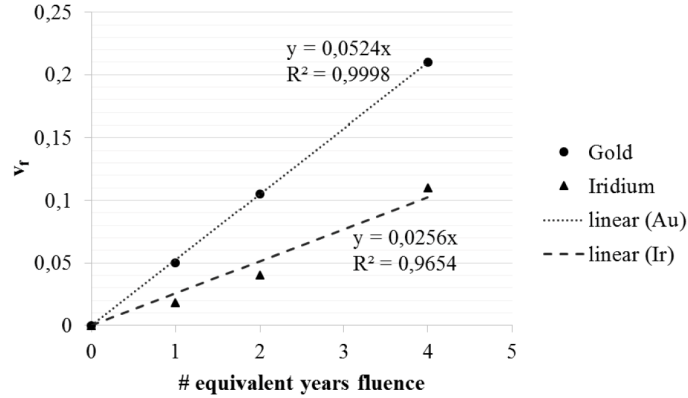


Fig. 13. Volume fraction inserted in the model in order to verify the relative reflectivity loss experimentally observed.

A linear relation between the volume fraction inserted in the model to predict experimental R drop and the fluence is confirmed. This endorses the validity of the model adopted to explain the main effects of the He + ions implantation. We can therefore state that the main effect is to change locally, in the region of implantation, the metal optical constants because of voids in the structure where the helium atoms are implanted decreasing in this way the overall density of the film. This is also consistent with the change in density adopted to better fit the gold SRIM curve, see Fig. 8.

#### 4. Conclusions

The effects of low energy He + on metal mirrors (gold, iridium) have been investigated simulating the effect of solar wind ions on optical coatings during long-term missions operating in the environment close to the sun. The overall reflectance decreases with increasing the total fluence of irradiation in almost all spectral ranges investigated, except particular regions where plasmonic effects at the surface may occur. SIMS measurements confirmed in fact that helium is implanted in a region below the surface. The change in reflectance can be explained by considering a thin intermixing layer under the surface, located in correspondence of the He depth profile estimated by SIMS, in which the density of the material is reduced. The model shows that reflectivity decreases linearly with the total fluence, demonstrating that the effect of low energy ions irradiation represents a modulation of the refractive index. This effect is more dramatic at shorter wavelengths and it is more pronounced in the case of gold. Such results demonstrate that it is necessary to deeply investigate the effect on different materials, selecting best candidates to withstand such environmental agents. The development of strategies to avoid the degradation of optical components, to mitigate it, or to re-generate the optics in space is a fundamental step for obtaining robust and truthful scientific data in space observations..

#### Acknowledgments

The authors thank Dr. A. Giglia and Prof. S. Nannarone for measurement at ELETTRA-BEAR beamline, the SPIRIT technical and administrative staff of the Forschungszentrum Dresden-Rossendorf for support during ion implantation experiment, Prof. Antonucci, METIS PI, Dr. Silvano Fineschi and G. Naletto, METIS Responsible. This work has been performed with the financial support of the Italian Space Agency (ASI/INAF/015/07/0 and ASI/INAF/Solar Orbiter) and of the Cassa di Risparmio di Padova e Rovigo (CARIPARO) Foundation, Bandi di Eccellenza 2009/2010. This work has been supported by the European Community as an Integrating Activity “Support of Public and Industrial Research Using Ion Beam Technology (SPIRIT)” under EC contract no. 227012.